Deep-Sea Research I 100 (2015) 21–33

Contents lists available at ScienceDirect

Deep-Sea Research I

journal homepage: www.elsevier.com/locate/dsri

The distribution of benthic biomass in hadal trenches: A modelling approach to investigate the effect of vertical and lateral organic matter transport to the seafloor

Matteo C. Ichino [a,b,*], Malcolm R. Clark [c], Jeffrey C. Drazen [d], Alan Jamieson [e], Daniel O.B. Jones [a], Adrian P. Martin [a], Ashley A. Rowden [c], Timothy M. Shank [f], Paul H. Yancey [g], Henry A. Ruhl [a]

[a] National Oceanography Centre, University of Southampton Waterfront Campus, European Way, Southampton SO14 3ZH, UK
[b] Ocean and Earth Science, National Oceanography Centre, Southampton, University of Southampton Waterfront Campus, European Way, Southampton SO14 3ZH, UK
[c] National Institute of Water & Atmospheric Research (NIWA), Wellington 6021, New Zealand
[d] Department of Oceanography, University of Hawaii, Honolulu, HI 96822, USA
[e] Oceanlab, University of Aberdeen, Newburgh AB41 6AA, UK
[f] Department of Applied Ocean Physics and Engineering and Department of Biology (Bors and Shank), Woods Hole Oceanographic Institution, Woods Hole, MA, USA
[g] Biology Department, Whitman College, Walla Walla, WA 99362, USA

ARTICLE INFO

Article history:
Received 22 September 2014
Received in revised form
23 January 2015
Accepted 26 January 2015
Available online 19 February 2015

Keywords:
Hadal ecology
Sediment
Gravitational transport
Topography
Benthic biomass
Kermadec Trench

ABSTRACT

Most of our knowledge about deep-sea habitats is limited to bathyal (200–3000 m) and abyssal depths (3000–6000 m), while relatively little is known about the hadal zone (6000–11,000 m). The basic paradigm for the distribution of deep seafloor biomass suggests that the reduction in biomass and average body size of benthic animals along depth gradients is mainly related to surface productivity and remineralisation of sinking particulate organic carbon with depth. However, there is evidence that this pattern is somewhat reversed in hadal trenches by the funnelling of organic sediments, which would result in increased food availability along the axis of the trenches and towards their deeper regions. Therefore, despite the extreme hydrostatic pressure and remoteness from the pelagic food supply, it is hypothesized that biomass can increase with depth in hadal trenches. We developed a numerical model of gravitational lateral sediment transport along the seafloor as a function of slope, using the Kermadec Trench, near New Zealand, as a test environment. We propose that local topography (at a scale of tens of kilometres) and trench shape can be used to provide useful estimates of local accumulation of food and, therefore, patterns of benthic biomass. Orientation and steepness of local slopes are the drivers of organic sediment accumulation in the model, which result in higher biomass along the axis of the trench, especially in the deepest spots, and lower biomass on the slopes, from which most sediment is removed. The model outputs for the Kermadec Trench are in agreement with observations suggesting the occurrence of a funnelling effect and substantial spatial variability in biomass inside a trench. Further trench surveys will be needed to determine the degree to which seafloor currents are important compared with the gravity-driven transport modelled here. These outputs can also benefit future hadal investigations by highlighting areas of potential biological interest, on which to focus sampling effort. Comprehensive exploration of hadal trenches will, in turn, provide datasets for improving the model parameters and increasing predictive power.

1. Introduction

1.1. The effect of organic matter input on benthic biomass in the deep-sea

The main structuring factor for benthic diversity and biomass in the deep sea is believed to be food availability (Rex and Etter, 2010; Rex et al., 2006) while depth related hydrostatic pressure is likely a limiting factor for some fauna (Laxson et al., 2011; Yancey et al., 2014).

Abbreviations: LTM, Lateral Transport Model; ΔS, slope difference; *B*, burial; *c*, 50% transport efficiency threshold

* Corresponding author at: National Oceanography Centre, University of Southampton Waterfront Campus, European Way, Southampton SO14 3ZH, UK. Tel.: +44 7597508685.
E-mail address: matteo.ichino@noc.soton.ac.uk (M.C. Ichino).

http://dx.doi.org/10.1016/j.dsr.2015.01.010

Studies of the effects of food availability on deep-sea life typically rely on inferring relationships between measures of benthic biomass and organic matter. This organic matter is mostly synthesised in the euphotic zone, and subsequently exported by gravity to deeper waters. The export mainly takes place through three processes: (1) the vertical sinking of particulate organic carbon (POC, or marine snow), produced through photosynthesis in the euphotic zone (e.g., Sweetman and Witte, 2008); (2) the delivery of dissolved organic material through currents and other water movements (Bendtsen et al., 2002); and (3) the transfer of large amounts of organic matter through sinking of animal carcasses (Higgs et al., 2014; Lebrato et al., 2012; Smith and Baco, 2003). Furthermore, inorganic carbon can be fixed through chemosynthesis both on the seafloor (Olu et al., 1997) and in the water column (Middelburg, 2011). As particulate organic matter sinks to the seafloor, it is gradually re-mineralized (Martin et al., 1987; Suess, 1980) and POC fluxes decrease exponentially with depth; as a consequence, deeper parts of the ocean generally support lower levels of benthic biomass (Rex et al., 2006).

Food availability in the deep sea also varies spatially with latitude (Honjo et al., 2008) and distance from shore (Johnson et al., 2007), and temporally, via seasonality (Fabiano et al., 2001), inter-annual climate variation (Smith et al., 2013), upwelling of nutrient-rich waters (McGillicuddy et al., 1998) and natural iron fertilization (Venables et al., 2007). Benthic biomass is higher, and dominated by larger size classes, in areas of the deep-sea overlain by temperate waters than in those overlain by tropical seas (Galeron et al., 2000; Thurston et al., 1998). Similarly temporal reductions in food supply have also been observed to relate to smaller body sizes (Ruhl et al., 2008) and lower biomass (Ruhl et al., 2014).

Bathymetric characteristics may play an additional role in driving regional and local scale patterns in food availability. In areas of complex hydrodynamic activity, such as the summit of seamounts, the community structure can be dominated by suspension feeders and their predators, resulting in a biomass that is higher than might be expected from vertical fluxes alone (Rowden et al., 2010; Thresher et al., 2011). These observations suggest that, in these areas, input of organic matter through lateral advection, rather than vertical deposition of marine snow, may be the most important factor in determining standing stock (Clark et al., 2010; Duineveld et al., 2004).

1.2. Patterns of benthic biomass in hadal trenches

Hadal trenches are the deepest parts of the ocean. They are formed at subduction zones of oceanic plates, and they can extend to depths approaching 11,000 m (Gardner et al., 2014). While they make up a relatively small part of the ocean seafloor area (~1–2%), they account for 45% of the oceanic depth range (Jamieson et al., 2010). Hadal trenches are usually shaped as long and narrow valleys, and often run parallel to coastlines (e.g., Peru-Chile and Japan trenches) or an island arc (Philippine and Aleutian trenches). They are among the least studied habitats on the planet, and the factors that control the distribution and variation of their communities over time are poorly understood (Jamieson et al., 2010).

For more than 60 years, hadal explorations have mostly used grabs and trawls (Belyaev, 1989; Vinogradova et al., 1993), and these have only provided a qualitative description of the hadal ecosystem (Belyaev, 1989). Existing data suggest that hadal macro- and megafauna communities are dominated by beard worms (Family Sibligonidae), spoon worms (Order Echiuroidea), sea cucumbers (Order Holothuroidea) and pericarid crustaceans (Order Isopoda and Amphipoda). Other taxa, such as tunicates, cirripeds, bryozoans and sponges, are rarely collected in hadal samples. Furthermore, evidence from hadal explorations (Wolff, 1961), as well as from research on osmolytes (Kelly and Yancey, 1999; Yancey et al., 2014), suggests that fish cannot live deeper than ~8200 m (Jamieson and Yancey, 2012; Yancey et al., 2014). Depth appears also to limit the distribution of decapod crustaceans: these have been found in the Kermadec, Mariana and Japan trenches (Jamieson et al., 2009) at a maximum depth of 7703 m.

The general trends of decreasing biomass with increasing depth observed at bathyal and abyssal depths (Rex et al., 2006) are reduced and, in some cases, reversed in hadal trenches, where biomass appears to increase with greater depth (Danovaro et al., 2002; Wolff, 1970). This pattern can be spatially variable within a trench, as suggested by research in the Puerto Rico Trench where contrasting trends with depth occur in different areas (George and Higgins, 1979; Richardson et al., 1995; Tietjen et al., 1989), likely related to trench topography. The typical V-shape cross section of trenches may act as a funnel, and could convey the sediments laterally towards the axis (Itoh et al., 2011, Itou et al., 2000), and perhaps even along the axis towards the deepest points. More recent investigations, using benthic oxygen flux data, support the theory of higher deposition along the trench axis, as higher bacterial respiration has been recorded in trench sediments than in the surrounding abyssal plain (Glud et al., 2013).

In this paper we describe a modelling tool that could improve our understanding of benthic biomass in hadal trenches by accounting for the lateral transport of organic matter. The model is applied to the Kermadec Trench and the results can be used to make testable predictions about the relative distribution of benthic biomass within trenches which can be ground-truthed by future trench surveys. Moreover, any differences between model predictions and ground-truthed estimates could help constrain the degree to which other factors, such as currents, need to be taken into account.

2. Materials and methods

2.1. Modelling approach

A numerical model (Lateral Transport Model, LTM) was developed to estimate the benthic biomass of preselected benthic size classes in hadal trenches, as a function of both vertical and lateral down-slope transport of organic matter to the seafloor (Fig. 1). The model, written with the R language (R Core Team, 2012), had physical and biological compartments. In the physical compartment, fluxes of organic matter between cells were calculated

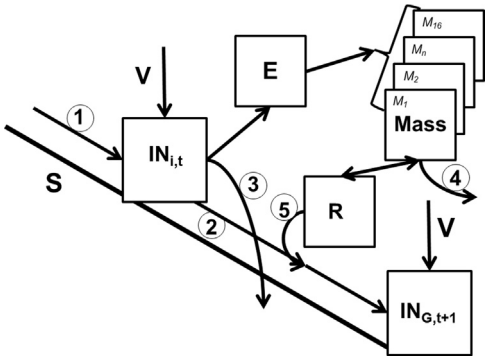

Fig. 1. Schematic diagram of the Lateral Transport Model (LTM). S=seafloor slope. V=vertical input of organic matter, obtained from Lutz et al. (2007) in this model application. 1=lateral input of organic matter from shallower cells. $IN_{i,t}$=total input flux in cell 'i' at time 't'. 2=lateral output flux towards deeper cells (G), which depends on slope steepness. 3=burial, or flux of organic matter into the sediment. This depends on the parameter B, which is the yearly burial rate. E=flux of organic matter available for consumption by benthic fauna. $Mass$=benthic biomass stock from 16 size classes (from M_1 to M_{16}) comprising macro- and megafauna. R=stock of organic matter resulting from mortality and defecation of benthic biomass (Mass). 4=loss of organic matter through respiration towards the water column. 5=flux of dead and defecated material towards deeper cells, depending on slope steepness. $IN_{G,t+1}$=total input flux in the deeper cells (G) at time '$t+1$'.

through matrix operations. In the biological compartment, a system of allometrically based differential equations (Kelly-Gerreyn et al., 2014) was used to calculate the biomass of 16 macro- and megafauna size classes utilizing the local organic detritus pool, which was fed by vertical and lateral POC fluxes. The size classes spanned from 0.12 g to 3.83 kg, and the nominal mass (geometric mean weight) of each class was double the previous one. Each cell received a constant (i.e. equilibrium) vertical input of POC at each time step (Lutz et al., 2007), as well as lateral fluxes from the neighbouring cells, determined by the slope. The organic detritus pool in each cell was used as food by the fauna and, using a size-based mortality rate, the organic matter was returned to the detrital pool and became available for lateral downslope transport.

The model relied on two input datasets: a 2D matrix of vertical input of POC ($g\,C\,m^{-2}\,y^{-1}$) converted to grams of wet weight, $g_{(ww)}$, by multiplying by a factor of 4, and a 2D matrix of the bathymetry of the area, which in this particular application was the Kermadec Trench, north-east of New Zealand. The bathymetric map used was obtained from GEBCO 30″ via the method "Resample (Data Management)" available through the software Arc Map 10 (ESRI, 2010); the new resolution of the map was 6' and the resampling type was "BILINEAR". The model was based on three key assumptions: (1) the lateral movements of sediment are controlled by gravity, or are approximated by gravity driven movement of particles down slope. (2) The POC has two sinks: one was physical, and was referred to as burial rate (B); the other was biological and accounted for energy loss through respiration (accounted for in the biological equations). (3) Scaling in the processes of growth, respiration, and mortality were determined by allometric relationships with body size (Kelly-Gerreyn et al., 2014). The effect of temperature on metabolic rates was not taken into account as this parameter was believed to be relatively constant (1–1.5 °C) throughout the trench (Blankenship et al., 2006; Jamieson et al., 2011).

For the purpose of our modelling exercise, we have not taken tectonic or chemosynthetic mechanisms into account as they are poorly known and thus difficult to quantify. From a geophysical point of view, hadal trenches are areas where oceanic crust is recycled in the Earth's mantle. This gives rise to extrusion of material and other tectonic events that could lead to extreme sediment fluxes in trenches (Itou et al., 2000). Geophysical activity such as the formation of hydrothermal vents or methane deposits could also influence animal community in the trench through processes of chemosynthesis supplementing available food supplies. There is insufficient information, however, to parameterize these influences in our model. Furthermore, the tectonic influences may be temporally rare and chemosynthetic inputs may be rather localised compared to the scale of the model.

2.2. Slope calculations

G was defined as the four cells surrounding i (the central cell of a moving window) in the four main directions (North, East, South and West): $G=\{N,E,S,W\}$.

First all slopes (S) between cells of the study area were calculated. In the general case of the slope between cell G and cell i, the slope was calculated as follows:

$$S_i^G = 2/\pi \arctan\frac{d_G - d_i}{cell} \tag{1}$$

where d_G is the depth of cell G, a negative value measured in meters; d_i is the depth of cell i, a negative value measured in meters; $cell$ is the resolution, or the width of the cell (~11,130 m at 6′ resolution), and $2/\pi$ is a factor to convert radians to a value between -1 and 1.

The result was a value that spanned between -1 (when G was deeper and the slope was vertical) and 1 (when i was deeper and the slope was vertical), 0 being a flat slope.

The relative slope in each particular direction was then defined as

$$\gamma_i^G = \frac{\left|S_i^G\left(1-D_i^G\right)\right|}{\sum_G\left|S_i^G\left(1-D_i^G\right)\right|} \tag{2}$$

where S_i^G is the slope between cell G and cell i (Eq. (1)), and D_i^G is a dummy variable which is 0 if the slope is negative, and 1 if the slope is positive.

Relative slope values were used for subdividing the lateral transport of sediment from one cell among the surrounding ones, as a proportion of the slope in each direction. If the four slopes going out of a certain cell were equal, the flux was equally divided between the directions. Similarly, if only some (or one) of the slopes were positive, the flux was directed in those (or that) directions.

2.3. Organic matter transport

The flux of bioavailable organic matter (E) that, in each cell (i) at any time-step (t), was available as food for the benthic community was defined as

$$E_{i,t} = (IN_{i,t} - OUT1_{i,t}) \times (1-B) \tag{3}$$

where $IN_{i,t}$ is the total input of organic matter in the cell (Eq. (4.1)); $OUT1_{i,t}$ is the fraction of input flux that was transported laterally as a consequence of slope steepness (Eq. (4.2)), and B is the burial rate, measured in % *per* year, including also the ingestion from other smaller size classes such as meiofauna and protozoa.

There were three fluxes of organic matter to i: (1) the vertical POC flux from the surface; (2) the lateral transport of POC from surrounding cells; and (3) the dead organic matter generated by the fauna in the surrounding cells (Fig. 1). These three sources were combined as follows to obtain the input and output:

$$IN_{i,t} = V_{i,t} + OUT1_{G,t-1} + OUT2_{G,t-1} \tag{4.1}$$

$$OUT1_{i,t} = \sum_G \gamma_i^G \times IN_{i,t} \times \tau_{S_i^G} \tag{4.2}$$

$$OUT2_{i,t} = \sum_G \gamma_i^G \times R_{i,t}/T \times \tau_{S_i^G} \tag{4.3}$$

where $V_{i,t}$ is the vertical input of POC, from Lutz et al. (2007); γ_i^G is the factor determining the possible directions (Eq. (2)); $IN_{i,t}$ is the input flux (Eq. (4.1)); $\tau_{S_i^G}$ is the transport efficiency value determined by the slope between i and G (Eq. (5)); $OUT1_{i,t}$ is the fraction of biological detritus that is transported laterally as a consequence of slope steepness; $R_{i,t}$ is the stock of sediment (biological detritus) present in the cell i at the time step t resulting from mortality and defecation (Eq. (7)), and $T=100$ d, residence time of organic sediments.

2.4. Lateral transport efficiency

An efficiency term (τ) limited the downslope fluxes of organic matter ($OUT1$ and $OUT2$). In the trenches the hydraulic forcing from currents and tides also likely plays a role in transporting and funnelling POC. However, we expected that gravitational forcing was likely to capture organic matter distribution patterns to a first approximation, and there was very little information on hydraulically driven POC fluxes in trenches or data on deep seafloor currents (Schmidt and Siegel, 2011). Therefore, at this stage, we limited model complexity to slope-driven fluxes.

The efficiency of lateral down-slope transport was expected to follow a logistic function (Bernhardt and Schultz, 2010; Bernhardt et al., 2012): low at gradual seafloor slopes and rapidly increasing at mid slopes until reaching 100% efficiency. This efficiency was

described by the following equation:

$$\tau = \frac{max \times (S \times 90)^a}{c^a + (S \times 90)^a} \quad (5)$$

where *max* is the maximum efficiency of down-slope transport. This parameter was set to 1, which resulted in down-slope transport of all available organic matter; a is a parameter that controls how quickly the efficiency changed from low to high; S is the slope between the cells (Eq. (1)), and c is the slope (°) at which τ was 50% of max.

The values of a and c affected the shape of the logistic curve in the following way: c affected the slope steepness at which τ is 50%, while a affected how fast τ changed with S at small slopes.

2.5. The biomass model

A simple model based on allometry (Kelly-Gerreyn et al., 2014) had been implemented in the LTM in order to estimate the benthic community biomass in each cell of the trench bathymetry. The model followed accepted allometric theory: biological processes such as ingestion, respiration, mortality and growth followed constant relationships with body weight across a broad spectrum of size classes. Furthermore, this model was considered relatively versatile, and had been successfully applied to three locations that differed in physical, chemical and biological characteristics: the Faroe-Shetland Channel in the north-east Atlantic, the Fladen Ground in the North Sea and the Oman Margin in the Arabian Sea (Kelly-Gerreyn et al., 2014). In this wide range of locations and conditions, the biological model provided a statistically similar and robust description of the data at each site, with only trivial changes to the parameters; therefore, we used a parameters-set that gave the best fit to the three above locations simultaneously, believing that it would yield comparatively useful approximations for the hadal zone.

In our application of the biological model, 16 size classes of hadal benthic macro- and megafauna ranged from 0.12 g to 3.83 kg, with doubling mass increments between size classes. This range had been chosen to represent a wide range of the possible contributors to the benthic biomass, both from the macro- and megafauna, and included the size class of the largest fish collected in the Kermadec Trench area (cusk eel *Spectrunculus* sp., ~3 kg) (Jamieson, personal communication), allowing for the presence of potentially rare large animals. In our model the benthic community 'grew' on a common detrital food pool (simulating a single trophic level), and performed the key processes of ingestion, respiration and mortality. This resulted in competitive interactions based on the allometric relationships, while predation was not explicitly accounted for in this model (Kelly-Gerreyn et al., 2014). While this was a simplified representation of ecosystem function, it should have provided a general snapshot of a particular benthic community from the point of view of the relationships between body size, biomass and abundance.

In the LTM, processes scaled with mean body mass, following basic allometric theory: after standardizing for the biomass of the animal, the rate of the processes decreased when the body weight increased (Griesbach et al., 1982; Peters, 1983). As a result, the value of biomass *per* size class was determined as

$$\frac{dMass_n}{dt} = 1 - r_n \times a \times g_n \times R_{i,t} \times Mass_n - m_n \times Mass_n^2 \quad (6)$$

where $Mass_n$ is the benthic biomass of the n^{th} size class; r is the respiration coefficient equal to $0.61M_n^{0.0046}$; a is the assimilation coefficient equal to 0.21; g is the ingestion coefficient equal to $1.76M_n^{-0.13}$; $R_{i,t}$ is the detritus (Eq. (7)); m is the mortality equal to $0.0009M_n^{-0.40}$; n is the size class number, and M_n is the nominal mass (geometric mean weight) of each size class (from 0.93 g to 3.06×10^4 g). Note that respiration rate was given by $r_n a g_n$ and so it decreased with M_n.

With this biomass model it was possible to estimate the mortality that occurred in each size class, which was then added to the detritus pool as an input. Therefore the detritus pool resulting from the mortality and defecation of the animals was calculated as

$$\frac{dR_{i,t}}{dt} = E_{i,t-1} - \sum_n a \times g_n \times R_{i,t} \times Mass_n + m_n \times Mass_n^2 \quad (7)$$

2.6. Tuneable parameters, sensitivity analysis and evaluation

We ran the LTM using the bathymetry of the Kermadec Trench area (between 25° and 38°S, and 174°W and 180°, Fig. 2), as this trench was

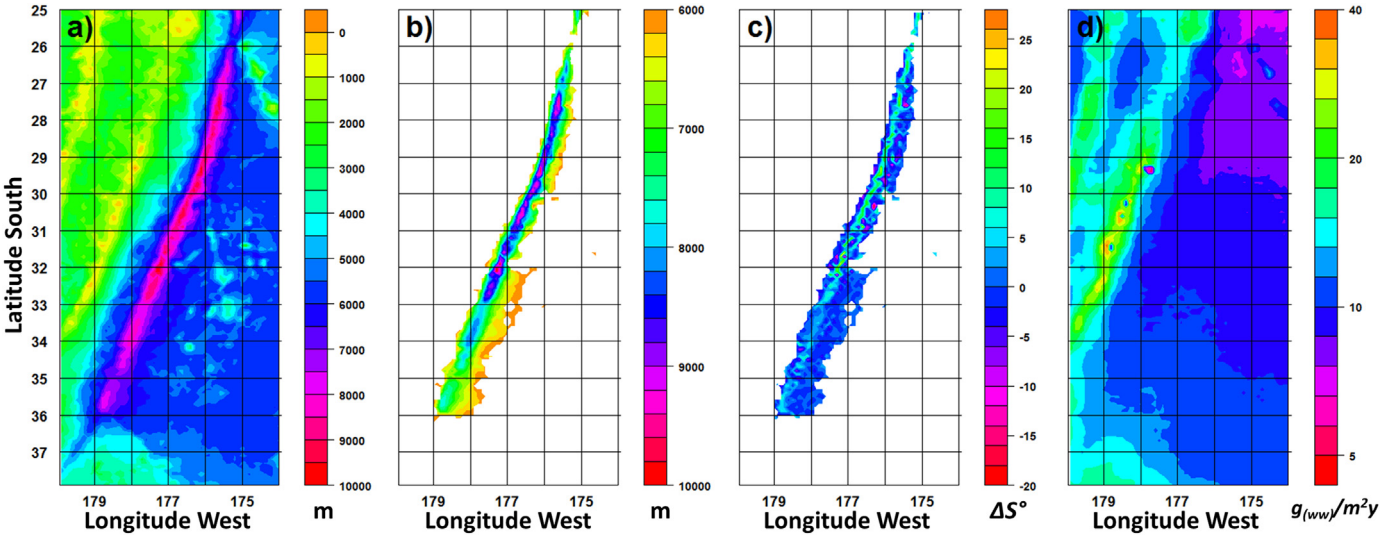

Fig. 2. Geographic domain of the model. (a) Bathymetric map of the Kermadec Trench region, on which the Lateral Transport Model (LTM) has been run. (b) The hadal area (> 6000 m depth) of the Kermadec Trench, isolated from the regional bathymetry. This map highlights the deep 'holes' found in the central and northern part of the trench, and the shape of the trench, which is wide in the southern part, and narrow in the northern part. (c) Slope difference (ΔS°) in the hadal area of the Kermadec Trench. This variable is calculated as the sum of incoming (positive) and outgoing (negative) slopes for each cell. As a result ΔS° is negative for the cells from which there mostly is export of organic matter, it is positive for the cells that mostly receive input of organic matter, and it is 0 for the cells that have similar inputs and outputs of organic matter. The deepest parts of the trench, located north of 32°S, are the areas with highest ΔS° values, while the southern parts of the trench, being wider and with more gentle slopes, have ΔS° values closer to 0. (d) Vertical input of POC at the seafloor, estimated by Lutz et al. (2007) for the Kermadec region, and multiplied by a factor of 4 to convert it from g C m^{-2} y^{-1} to g_{ww} m^{-2} y^{-1}.

among the better studied hadal areas of the ocean, focus of current research and characterized by intermediate levels of surface primary production (Longhurst et al., 1995). The Kermadec Trench had a relatively simple shape, being straight with a relatively constant slope gradient along the axis, with saddles separating increasingly deep basins towards the deepest point (~10,047 m). The western slope (fore arc) was steeper than the eastern slope. The southern end of the trench was ~160 km from the nearest land mass (New Zealand), and therefore likely to receive low fluxes of terrigenous materials relative to high levels of organic matter that have been observed in other trenches (e.g., Peru-Chile Trench, Danovaro et al. (2003)).

In order to explore the sensitivity of the LTM to variations of two independent variables, burial rate (B, Section 2.3, Eq. (3)) and transport efficiency (τ, and ultimately a and c, Section 2.4, Eq. (5)), we ran the model to equilibrium in five modes to provide examples of how these parameters related to each other. First keeping τ constant ($a=3$, $c=6^\circ$) and varying the value of B (4.5, 9 and 18% *per* year, covering the range of organic sediment burial suggested by Reimers et al. (1992) for a wide depth interval). Second, with $B=9\%$ *per* year, we varied the threshold of τ ($c=3^\circ$, $c=6^\circ$ and $c=12^\circ$), chosen as representative of the range of slopes present in the hadal trench (from 0° to 16°). The differences between the runs were measured by the response of four variables to variations of slope difference (ΔS): lateral organic matter input (Eq. (4.1)), buried organic matter, amount of organic matter available for ingestion (Eq. (3)) and resulting benthic biomass (Eq. (6)). These results were interpreted using two-way parametric ANOVA: main effects were ΔS (three levels) and the model scenario (either c or B, three levels each). Two-way parametric ANOVA was also used to interpret the effect of model scenario (either c or B, three levels each) by depth (shallow or deep) and topography (southern or northern part of the axis) on the modelled benthic biomass. In all the ANOVA tests the interactions between main effects were considered as well. All the analyses were done with the computer program R (R Core Team, 2012).

3. Results

3.1. Slope analysis

The mean slope in the hadal area of the Kermadec Trench (Fig. 2b) was 0.2° and the maximum was 16°. For the purpose of organic matter redistribution, the difference between incoming and outgoing slopes (one from each direction G) for each cell determined whether the organic matter was mostly exported from the cell (local maxima in the bathymetry, such as the summit of underwater hills and seamounts, with negative slope difference values) or imported (local minima in the bathymetry); this will be referred to as slope difference (ΔS). The frequency distribution of ΔS° was normal, with a mean of 0°, ranging between −19.5° and 27.6° (Fig. 3).

The LTM was run under five scenarios, where the varying parameters were burial rate (or uptake inefficiency) ($B=4.5$, 9 and 18% *per* year), and downslope transport efficiency (50% efficiency (c) at 3°, 6° or 12° of steepness). Lateral organic matter inputs, burial of organic matter and available organic matter from which the benthic fauna depended, all had a positive relationship with the main effect ΔS (three levels: negative, zero and positive); although the outputs changed only marginally when varying B, they were strongly affected by variations of c.

3.2. Slope and levels of lateral sediment input, burial, available sediment and benthic biomass

Lateral organic matter input (Fig. 4, Table 1 and Table A.1): Lateral organic matter input increased with ΔS when c was held constant

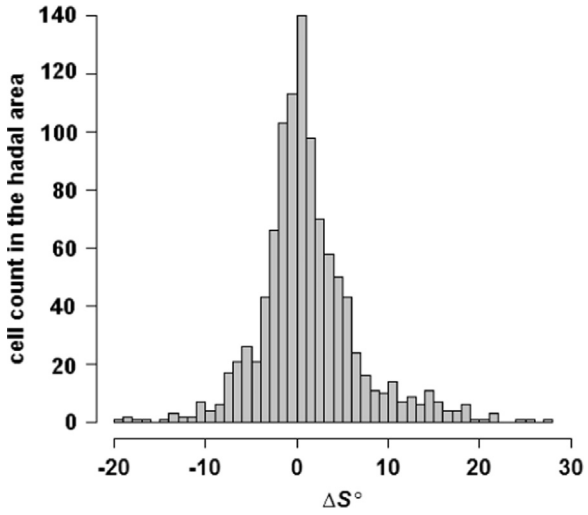

Fig. 3. Slope difference cell counts in the hadal area of Kermadec Trench. The slope difference is the net quantification of the amount of slopes towards and from each cell; therefore it is negative in the local maxima (hills and seamounts) and positive in the local minima (bottom of depressions). The frequency distribution is centred on cells with slope difference of 0°, therefore cells with equal inputs and outputs. These can be flat, or sloping.

while there was no main effect from B. When B was held constant, there was interaction between c and ΔS in determining the increasing trend of lateral organic matter input; as a consequence lateral organic matter input increased more strongly from areas with negative ΔS to areas with positive ΔS when the transport efficiency was high ($c=3^\circ$), rather than when it was low ($c=12^\circ$).

Burial of sediment (Fig. 4, Table 1 and Table A.1): With constant $c=6^\circ$, the amount of annually buried organic matter *per* cell was positively affected by an interaction of ΔS and B. Similarly ΔS and c had an interacting effect on the amount of annually buried organic matter *per* cell when B was held constant.

Mass of available food (Fig. 4, Table 1 and Table A.1): When c was held constant, both B and ΔS (main effects) had a significant effect on the amount of available food in each cell: this increased with ΔS, and decreased with the level of B. When B was held constant, ΔS and c had an interacting effect on the mass of available food. As a consequence, in cells with negative ΔS, available food was highest under low c conditions and lowest under high c conditions, while the scenario was reversed in cells with positive ΔS.

Biomass of fauna (Figs. 4 and 5, Table 1 and Table A.1): The biomass of benthic fauna in the hadal area of the Kermadec Trench significantly increased with ΔS when c was held constant, and there was also a small but significant positive effect from the increase of B. When B was held constant, ΔS and c had an interacting positive effect on benthic biomass. The relationships between benthic biomass, slope difference and parameter sets were used to derive maps of expected benthic biomass in the Kermadec Trench area (Fig. 5). Two characteristics stood out from these plots; the first was the relative similarity between (a), (b) and (c), which suggested that variations of B have a small effect on biomass; by contrast the large differences between (d), (b) and (e) suggested the relative importance of transport efficiency threshold (c) in determining the distribution of biomass. Substantial differences in spatial heterogeneity of biomass were also apparent between the differing transport efficiency thresholds: at low levels of transport efficiency (Fig. 5e) predicted biomass decreased gradually northwards, possibly as a consequence of lower POC input towards the more oligotrophic (tropical) parts of the trench. When the transport efficiency was higher (Fig. 5d), predicted biomass was higher along the axis and lower along slopes of the trench.

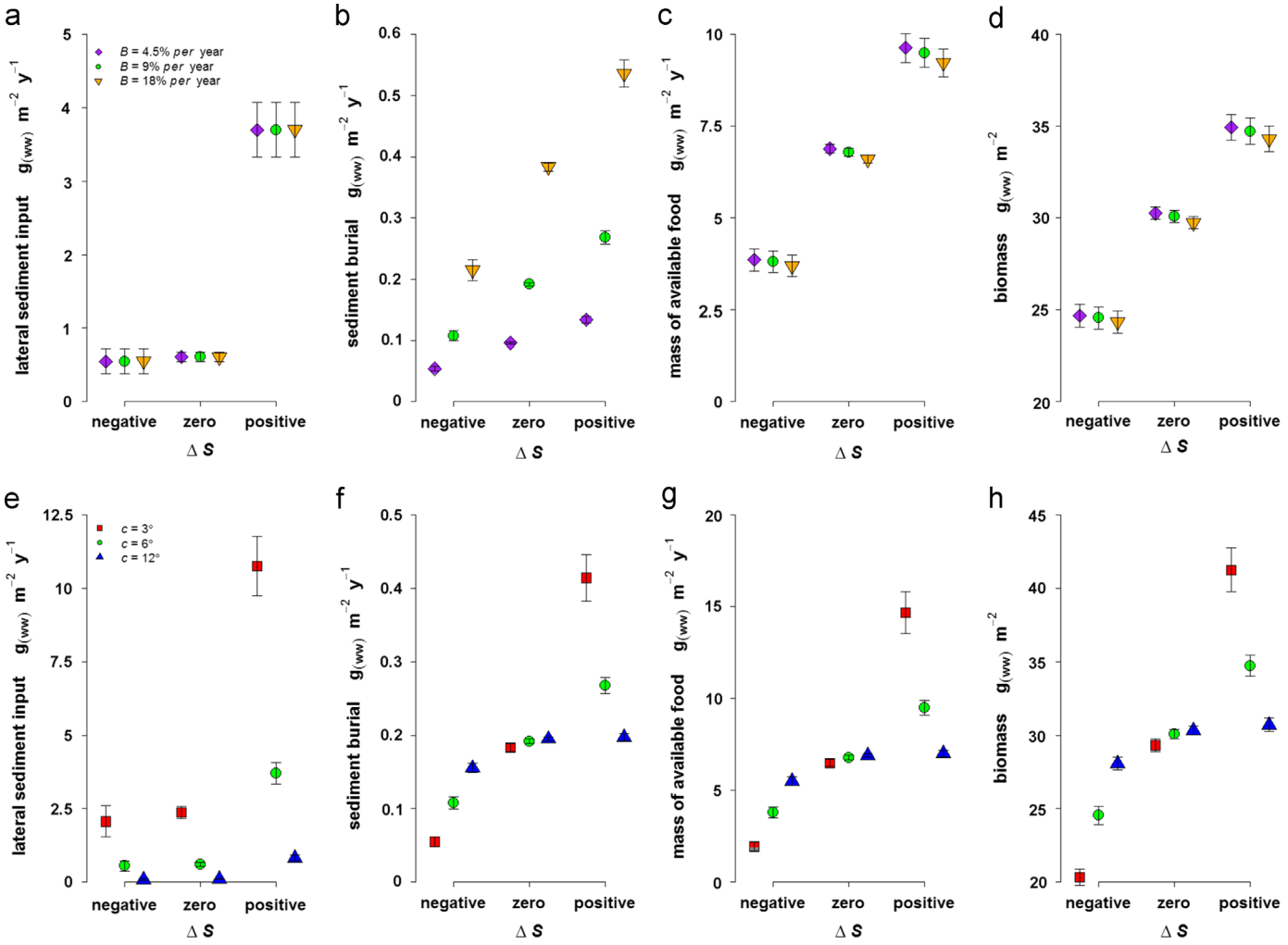

Fig. 4. Variation of four modelled response variables with the slope difference (ΔS) in the hadal area of the Kermadec Trench. Error bars show 95% confidence intervals. The first row of plots (a–d) summarizes the results from model runs in which the burial rate (B) varies between 4.5% and 18% *per* year. The second row of plots (e–h) summarizes the results from model runs in which the transport efficiency threshold (c) varies between 3° and 12°. (a) and (e) lateral input in each cell; (b) and (f) burial of sediment; (c) and (g) sediment available for ingestion; (d) and (h) benthic biomass. The responses are measured in five different model settings represented with different symbols and colours. All the response variables have a positive relationship with ΔS. When B is modified, the response variables show only small variations, while large variations of the response are recorded when c is changed.

Table 1
F values and statistical significance obtained from testing the effect of ΔS and model scenario on four outputs of the LTM, through eight ANOVA tests. (a) The level of slope difference (ΔS=negative, zero or positive) always has a statistically significant effect on the model outputs when lateral transport efficiency threshold is held constant (c=6°), while the level of burial rate (B=4.5, 9, 18% y^{-1}) does not appear to significantly affect the lateral sediment input. Only for the model output "sediment burial" there is significant interaction between ΔS and B. (b) When the burial rate is held constant (B=9% y^{-1}), all four model outputs are affected significantly by an interaction of ΔS (ΔS=negative, zero or positive) and level of lateral transport efficiency threshold (c=3°, 6°, 12°). The degrees of freedom of the residuals are 3114 for each test. Significance codes used: 0 '***' 0.001 '**' 0.01 '*' 0.05.

(a)	**ΔS (df=2)**	**Level of B (df=2)**	**Interaction (df=4)**
Lateral sediment input	1208.6 ***	0.0	0.0
Sediment burial	768.5***	5286.2***	109.8***
Mass of available food	987.7***	7.4***	0.2
Biomass	508.2***	3.6*	0.0
(b)	**ΔS (df=2)**	**Level of c (df=2)**	**Interaction (df=4)**
Lateral sediment input	691.9***	665.1***	215.4***
Sediment burial	699.1***	20.4***	221.9***
Mass of available food	699.1***	20.4***	221.9***
Biomass	483.4***	1.4	127.6***

Higher levels of food availability, estimated to occur at the local minima of the bathymetry, affected the total benthic biomass estimate but not the relative abundance of the size classes (Table A.2). Density increased consistently across size classes when food availability increased, and this could be quantified by taking as reference point the density of 1 ind. m^{-2}: with higher food input, bigger individuals could reach this reference density. This allowed suggesting that the community composition changed with food availability, as the presence of larger size classes was supported by higher food availability.

3.3. Trench depth, shape and axis topography

Benthic biomass increased with depth under all model scenarios apart from the one with low transport efficiency (Fig. 6 and Table 2). When c was held constant (Fig. 6a) the modelled biomass was positively affected by increasing depth, while there was no effect from the level of B. When B was held constant (Fig. 6b), transport efficiency and depth interval interactively affected the variation of biomass: the response was similar between levels of c up to 8500 m, while in the deepest parts of the trench biomass increased strongly with high transport efficiency values and decreased with low c.

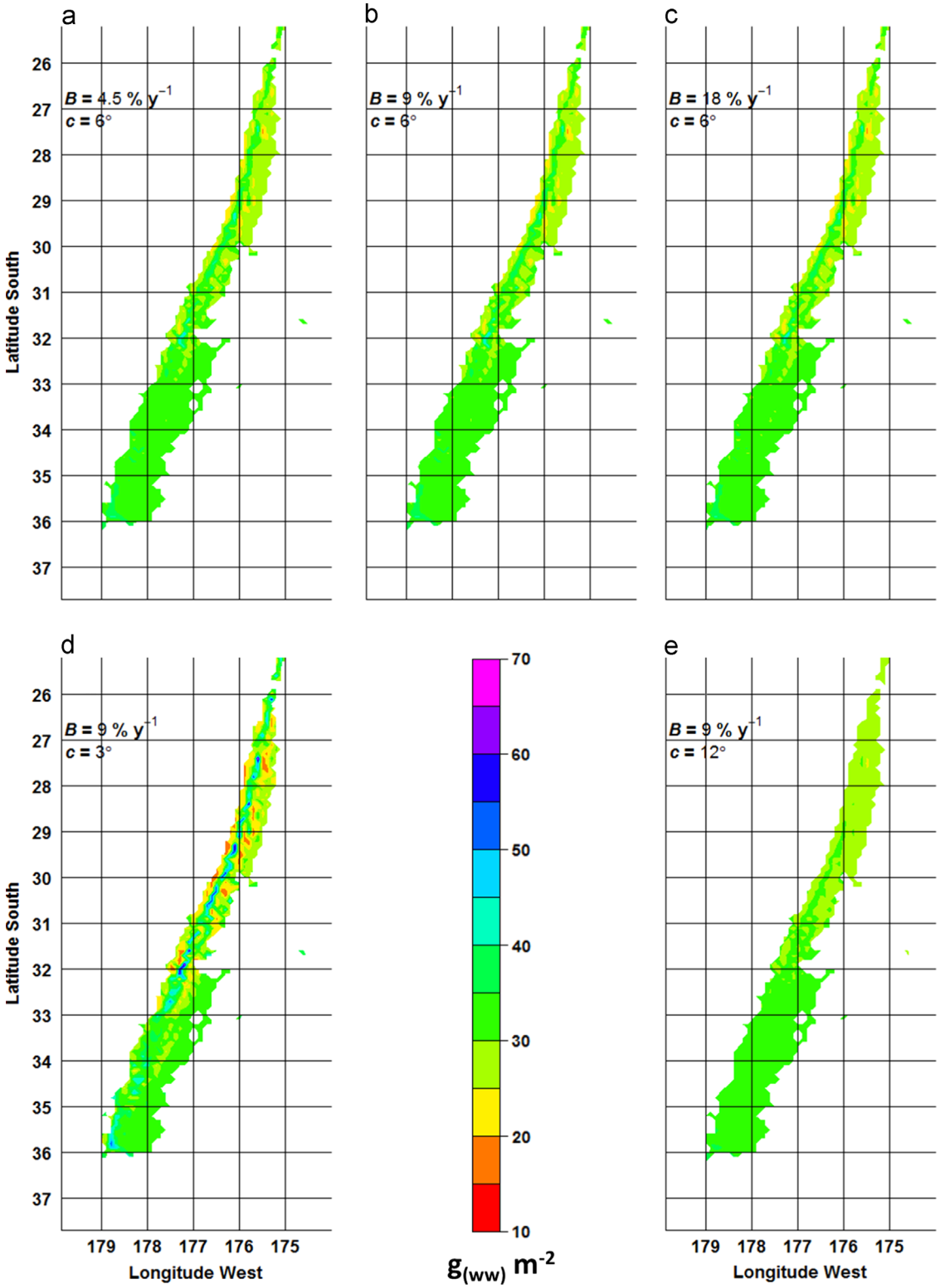

Fig. 5. Maps of the distribution of benthic biomass ($g_{(ww)}\ m^{-2}$) in the hadal area of the Kermadec Trench. The five maps show results from five runs of the Lateral Transport Model (LTM) under five combinations of burial rate (B) and transport efficiency threshold (c). In the top three maps c is held constant (6°), while B is increased from 4.5% y^{-1} to 9% y^{-1} and 18% y^{-1}. In the two bottom maps B is held constant at 9% y^{-1}, while c is changed from low slope values (3°) to high slope values (12°). Two characteristics stand out from these maps; the first is the relative similarity between (a), (b) and (c), which suggests that B has a small effect on benthic biomass; by contrast the differences between (d), (b) and (e) suggest the high importance of transport efficiency threshold in determining the distribution of benthic biomass.

Together with depth, trench topography played a role in determining benthic biomass patterns in the model. Depth increased along the axis of the Kermadec Trench, from south to the centre of the trench, with a relatively constant slope gradient, until reaching ~8500 m (Fig. 7). In the southern part of the axis the modelled benthic biomass was relatively low and it decreased towards the mid part of the axis under all model conditions (Fig. 7a and b, Table 3). Such behaviour changed in the central and northern parts

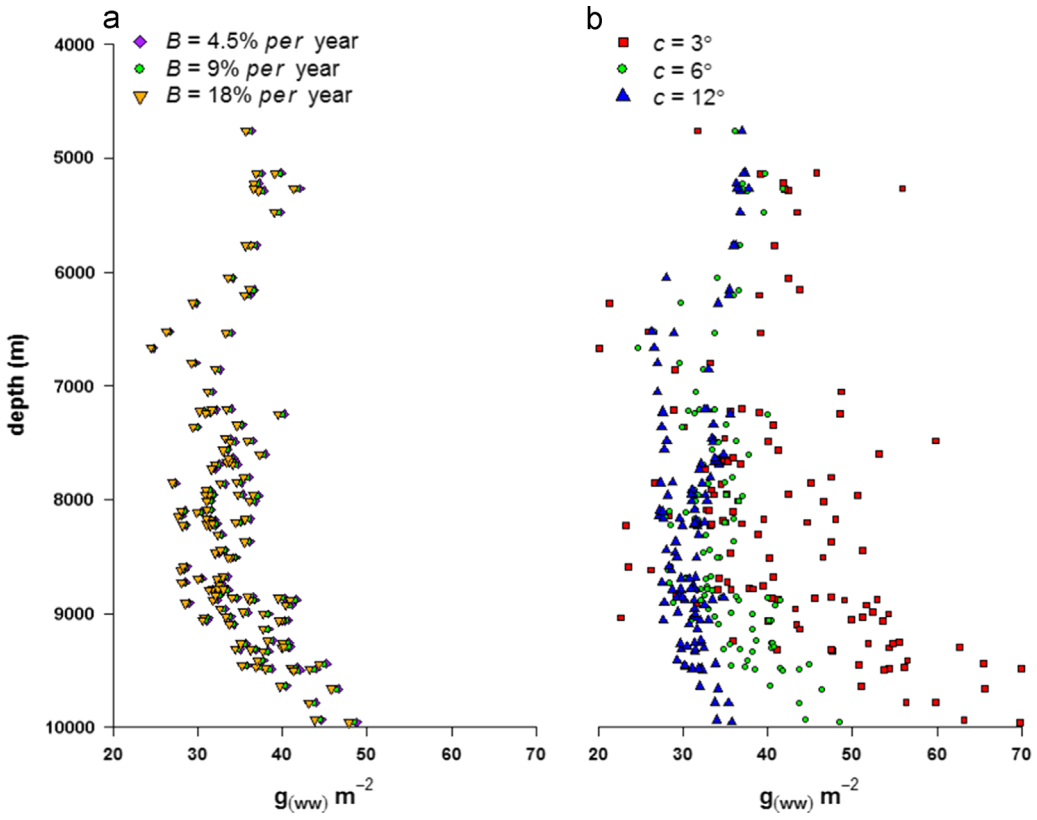

Fig. 6. The increase of benthic biomass ($g_{(ww)}\ m^{-2}$) with depth along the axis of the Kermadec Trench. The benthic biomass was predicted through five runs of the LTM, with different levels of burial rate (B, panel a) and transport efficiency threshold (c, panel b) represented with different symbols and colours. The benthic biomass increase with depth is small in the shallow part of the trench (down to 8500 m) and stronger in the deep part of the trench (deeper than 8500 m). The response differs between model runs only between different levels of c, while different levels of B do not result in significantly different outputs.

of the axis where the biomass was much more variable. When B varied and c was constant (Fig. 7a), the biomass did not change significantly along the axis between the northern and southern areas. However, when c varied and B was kept constant (Fig. 7b) the two main effects (position along the axis and transport efficiency threshold) interacted resulting in a higher difference in the modelled biomass between the northern and southern parts of the axis.

Overall, slope and topography affected the accumulation of organic sediment (and biomass) resulting in patterns that would not have been expected if only the vertical flux of organic carbon from the ocean surface was taken into account (Fig. A.3). Under high levels of lateral transport efficiency up to twice as much biomass was found in areas with positive ΔS° than would be expected in the absence of lateral transport, and up to half as much biomass in areas with negative ΔS°. Furthermore, the process of lateral transport caused biomass levels in areas of net sediment input (deepest holes along the axis, especially in the central and northern parts) to be between two and four times higher than in areas of net sediment output.

Table 2
F values and statistical significance obtained from testing with two ANOVAs the effect of depth and model scenario on the benthic biomass estimated through the LTM. When transport efficiency is constant ($c=6^{\circ}$) the depth factor (shallow vs. deep) causes a significant increase of benthic biomass, while there is no effect from changing the level of burial rate ($B=4.5$, 9, 18% y^{-1}). When the burial rate is held constant ($B=9\%\ y^{-1}$), depth factor and transport efficiency threshold ($c=3^{\circ}$, 6°, 12°) have an interacting effect on the modelled benthic biomass. This increases with increasing depth under high and intermediate levels of transport efficiency, while it decreases with depth when the transport efficiency is low ($c=12^{\circ}$). The degrees of freedom of the residuals are 357 for each test. Significance codes used: 0 '***' 0.001 '**' 0.01 '*' 0.05.

	Depth factor (df=1)	Model scenario (df=2)	Interaction (df=2)
Varying B, constant c	59.0554***	0.7349	0.0031
Varying c, constant B	34.726***	93.553***	16.822***

4. Discussion

We have presented a model that estimates biomass of benthic fauna as a consequence of vertical and lateral organic matter inputs. The results provide testable hypotheses for elucidating the potential effects of local topography on benthic biomass distribution in trench environments. To our knowledge, this is the first such model for deep-sea habitats, and we believe that it can be used to improve our understanding of benthic ecology in relation to topography.

In our framework, the effect of local topography (ΔS) on biomass, and its consequent spatial distribution, was mostly dependent on transport efficiency (c), while burial rate of organic sediment (B) did not appear to have a strong effect. The relative insensitivity of the model to changes in the burial rate suggests that constraining the residence time of sediments, which appears to be highly variable and dependant on sediment type (Mayor et al., 2012), would only slightly improve the accuracy of model predictions. In areas of negative ΔS (hills or high areas) the biomass was higher under high c scenarios (low transport efficiency), while this pattern was reversed in areas of positive ΔS (depressions, or the trench axis). Future attempts to fully evaluate this model should therefore be aimed at measuring the

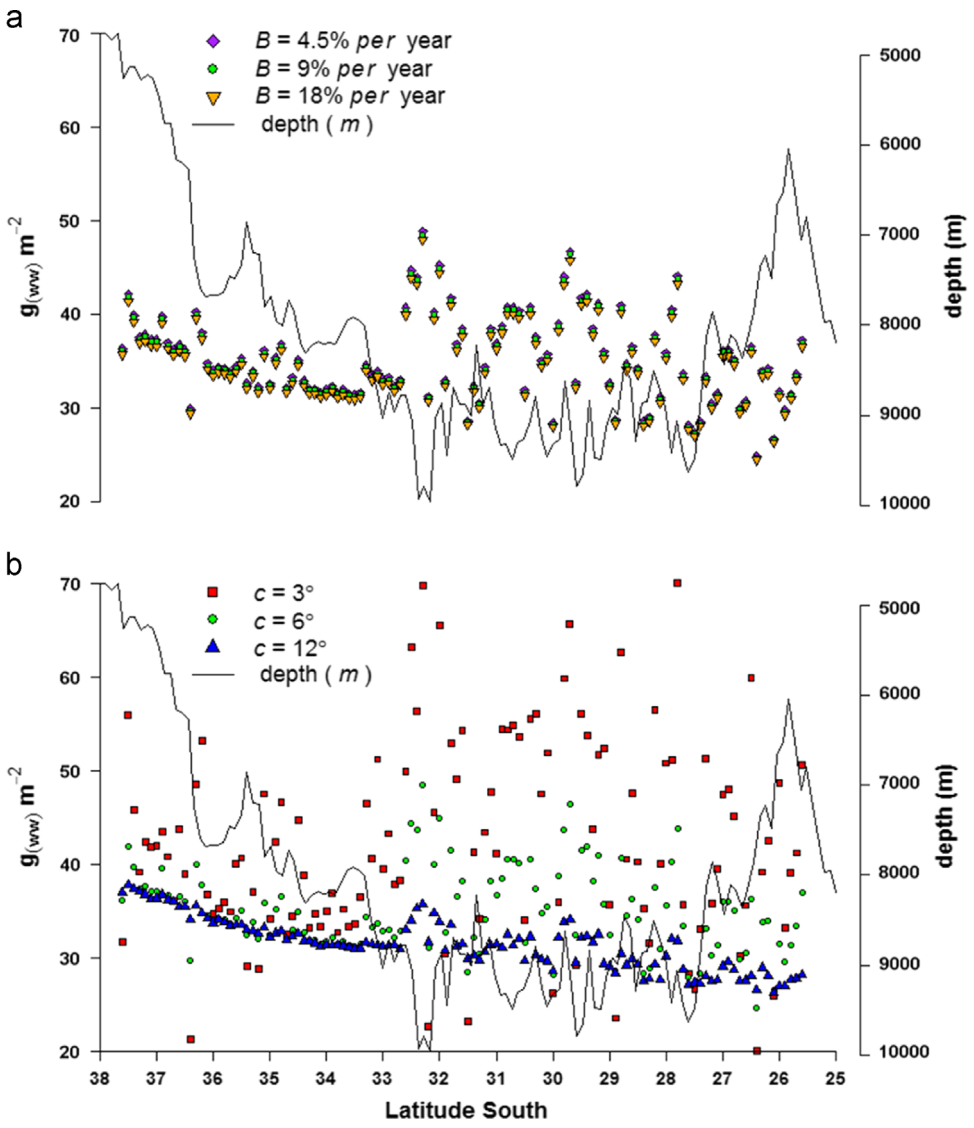

Fig. 7. Benthic biomass along the axis of the Kermadec Trench, under 5 different sets of parameters. Depth profile along the axis of the trench is superimposed to both panels and measured on the right-hand-side y axis. From the south the depth increases at a constant rate up to ~8500 m, after which it fluctuates around this value, before decreasing towards the north. (a) Benthic biomass along the axis of the Kermadec Trench, as predicted from the LTM keeping transport efficiency threshold constant (c=6°) and varying burial rate (B=4.5, 9 and 18% *per* year). (b) Benthic biomass along the axis of the Kermadec Trench, as predicted from the LTM keeping burial rate constant (B=9% *per* year) and varying transport efficiency threshold (c=3, 6 and 12°). The benthic biomass is low and constant in the southern part of the trench, where the depth increases, and then it becomes highly variable in the central and northern areas of the axis, where the trench is narrower with steeper slopes (Fig. 2).

Table 3
(a) Mean and standard deviation of benthic biomass ($g_{(ww)}$ m^{-2}) in the southern and central part of the Kermadec Trench axis, measured under five LTM scenarios with different levels of sediment burial rate (B) and the transport efficiency threshold (c). (b) F values and statistical significance obtained from testing with two ANOVAs the effect of location (north vs. south) and model scenario on the benthic biomass estimated through the LTM. When transport efficiency is constant (c=6°) benthic biomass does not change significantly with location nor with burial rate (B=4.5, 9, 18% y^{-1}). When burial rate is constant (B=9% y^{-1}) benthic biomass is affected interactively by location and transport efficiency threshold (c=3°, 6°, 12°). When the transport efficiency is high (3°) benthic biomass increases from south to north, while when transport efficiency is low (12°) benthic biomass decreases from south to north. The degrees of freedom of the residuals are 357 for each test. Significance codes used: 0 '***' 0.001 '**' 0.01 '*' 0.05.

(a)	**South**	**North**	***t*-Test (*p*-value)**
B=4.5% y^{-1}; c=6°	34.6 (0.4)	35.5 (0.6)	−1.22 (0.2265)
B=9 % y^{-1}; c=6°	34.4 (0.4)	35.3 (0.6)	−1.22 (0.2259)
B=18% y^{-1}; c=6°	34.0 (0.4)	34.9 (0.6)	−1.22 (0.2246)
B=9% y^{-1}; c=3°	38.7 (1.0)	44.4 (1.4)	−3.37 (0.0010)***
B=9% y^{-1}; c=12°	33.5 (0.3)	30.1 (0.3)	6.30 (3.919e−13)***
(b)	**Location (df=1)**	**Model scenario (df=2)**	**Interaction (df=2)**
Varying B, constant c	2.9043	0.6357	0.0001
Varying c, constant B	2.0825	84.9628***	13.6145***

benthic biomass in areas with a wide range of ΔS, as this would help determine a more accurate value for c. The current application of the model was intended only to provide general trends between benthic biomass and ΔS, depth and trench shape, and used the Kermadec Trench as an example area. Model outputs included maps of the expected biomass distribution for this area of interest. Such maps can be used for survey planning as they provide an overview of the biomass patterns theoretically induced by local topography.

In the Kermadec Trench, under all sets of parameters, the model predicted an accumulation of organic matter and benthic biomass along the axis of the trench, and depletion on the surrounding slopes. The benthic biomass levels were predicted to be up to twice as high in the central and northern parts of the trench, where the axis reaches greater depths, and the trench is narrower with steeper slopes. In the southern part of the trench the slopes are gentler; as a consequence the biomass was predicted to change only marginally between the slopes and the axis. This prediction is opposed to what would be expected as a consequence of the surface primary production and vertical POC flux. As the trench runs in a south-north direction from temperate to sub-tropical regions it receives a gradient of POC flux decreasing from south to north. This gradient, which is likely to have a strong effect on the ecology at the ocean surface, may not translate to areas within the trench where lateral fluxes become important. The response of benthic biomass to ΔS does not change when it is standardized by the vertical flux (V), suggesting that ΔS, rather than vertical sediment input, drives the biomass distribution in the model. In case of extremely low lateral transport efficiency ($c=12^\circ$) the benthic biomass across the whole hadal area is lower than it would in the absence of lateral transport. This result suggests an interaction between lateral transport and burial rate that results in lower fluxes of biologically available sediment (E).

Accumulation of organic sediments and biomass along the axis of the trench can be similar to that found along the axis of submarine canyons, where organic matter and benthic biomass levels are generally higher than on the surrounding slopes (Vetter and Dayton, 1998). Strong currents along the axis of canyons (up to 1.9 m s^{-1} in the Scripps Canyon) are generally suggested as a reason for organic matter accumulation along the axes (Inman et al., 1976). There is no evidence that trenches experience the kind of intense cascading currents seen closer to shore at shallower depths (e.g., Canals et al. (2006)), and hence gravitational transport may provide a useful first approximation in trenches. The few empirical measurements from hadal trenches suggest that typical current speeds for these regions are low (on the order of 1 cm s^{-1} in Puerto Rico Trench Schmidt and Siegel, 2011, and 16.2 mm s^{-1} $\pm$ 8.5 in the Kermadec Trench Jamieson et al., 2013). Furthermore, the effect on sediment redistribution of water mass movements around deep-sea topographic features is complex (Turnewitsch et al., 2013), and would need to be addressed with a significantly more complex modelling approach. Even though the effective sinking speed is limited by the time step interval, grid spacing, slope and transfer efficiency applied, the model results are insensitive to variations in time step and grid spacing because the model is run to equilibrium, as confirmed by a sensitivity analysis. In the future, better understanding of effective speed and slope transport may allow for improvement in this aspect of our model framework.

High-frequency fluid dynamics may have an important effect on sediment distribution at hadal depths, as suggested by research in north-western Pacific trenches (Turnewitsch et al., 2014); areas with high internal tides intensity have sediment deposition that is lower than expected, possibly as a consequence of particle break-down and consequent re-suspension or lower sinking rate. Also, abrupt events such as earthquakes (Itou et al., 2000) can induce extreme levels of sediment and associated organic matter transport in hadal trenches. Cyclones could have similar effects in trenches that are close to land masses, as they increase the input of terrestrial organic materials in the water column, which can then be transported to depth (George and Higgins, 1979). We did not attempt to take either of these latter effects into account, but we acknowledge that they exist and that future research could consider them.

Distance from land is, potentially, another relevant factor in determining the amount of lateral sediment fluxes to a trench. High meiofauna abundance in the Puerto-Rico and Atacama trenches have been attributed to inputs of terrestrial organic materials (Danovaro et al., 2002; Tietjen et al., 1989); similarly abundance, species richness, and diversity appear to be higher in the New Britain Trench, rather than in the Mariana Trench, possibly as a consequence of higher allocthonous food input (Gallo et al., 2015); furthermore, distance from land has been found to influence the meiofauna abundance and community composition in Mediterranean non-hadal trenches off the Greek coast (Tselepides and Lampadariou, 2004). A factor accounting for distance from shore could probably improve model interpretations when comparing multiple trenches.

ΔS could be an effective indicator of organic sediment matter accumulation from lateral transport in the Kermadec Trench, and could explain some of the benthic biomass patterns found in other hadal trenches. Meiofauna biomass and abundance in the Puerto-Rico Trench, recorded by Tietjen et al. (1989), were higher at the deep station (8189 m) than at the shallow station (7394 m). With a simple slope analysis for these two areas through the GEBCO bathymetry, we find that the deep station is in an area of net organic matter input, having positive ΔS, while the shallow station is an area of net organic matter output (Table 4). Therefore, according to our model the two stations would have different organic matter accumulation rates, which could explain the different levels of observed meiofauna biomass and abundance (Tietjen et al., 1989). In the same trench, George and Higgins (1979) investigated the macrofauna biomass and abundance at Brownson (8800 m) and Gillis Deep (7600 m) sites, finding that both were higher at the shallower station.

They suggested that this was caused by the input of plant debris through a submarine canyon at Gillis Deep, something we cannot

Table 4
Comparison of literature data with ΔS° predictions through the GEBCO 6' bathymetry.

Reference	Site name	Trench name	Lat	Long	Depth (m)	GEBCO depth (m)	ΔS°	Meiofauna		Bacteria
								Abundance ind. /10 cm^2	Biomass µg C/10 cm^2	Respiration
Tietjen et al. (1989)		Puerto-Rico	19°08.7′N	66°14.3′W	7460	7394	−2.37	44 (± 10)	3.8 (± 1.6)	
Tietjen et al. (1989)		Puerto-Rico	19°35.7′N	66°11.2′W	8189	8373	4.30	96 (± 15)	14.3 (± 5.1)	
Danovaro et al. (2002)	B1	Atacama	23°30.5′S	70°42.8′W	1050	2359	3.78	550 (± 186)	1053 (± 140)	
Danovaro et al. (2002)	B4	Atacama	23°46.6′S	70°34.4′W	1140	1733	6.74	672 (± 350)	578 (± 239)	
Danovaro et al. (2002)	C7	Atacama	23°15.0′S	70°40.0′W	1355	2324	0.26	639 (± 425)	723 (± 534)	
Danovaro et al. (2002)	A1	Atacama	23°15.0′S	71°21.0′W	7800	7592	13.03	6378 (± 3061)	824 (± 348)	
Glud et al. (2013)	Reference	Mariana	10°50.8′N	142°33.8′E	5982	6531	1.75			Low
Glud et al. (2013)	Challenger deep	Mariana	11°22.1′N	142°25.8′E	10,813	9494	6.38			High

confirm with our model framework yet, as the station location data are not precise enough. In the Peru-Chile Trench there are meiofauna hotspots at a depth of 7800 m supported by high concentrations of nutritionally rich organic matter (Danovaro et al., 2002). This site has a higher ΔS° value than the other sites examined by Danovaro et al. (2002) (Table 4). More recently, Glud et al. (2013) suggested elevated rates of organic matter inputs as the cause of higher concentration of microbial cells and higher oxygen consumption at Challenger Deep in the Mariana Trench, when compared to a site on the neighbouring abyssal plain (Reference site). Also in this case the ΔS° estimated through the GEBCO bathymetry is higher for the suggested high-deposition site (Table 4). Glud et al. (2013) also found that bacterial respiration in the deepest point of the Mariana Trench was about twice that on the adjacent abyssal plain. For the Kermadec Trench we found a similar result, as the modelled biomass in the areas of highest input, under high transport conditions (B=9% y^{-1}, c=3°) can be up to two times higher than with no transport. Furthermore, under almost all model scenarios we found that the local minima in the trench bathymetry have higher biomass levels than would be expected without transport.

There are few quantitative data of benthic fauna biomass/abundance currently available for the Kermadec Trench and these data are mainly from sampling expeditions in the 1950s (Belyaev, 1989). These data are insufficient to fully validate the model. Nevertheless Belyaev (1989) noted that of the two trawl stations of the *Vityaz* expedition, benthic biomass was estimated to be slightly higher at the deepest site (0.06 g m^{-2} at ~10,000 m compared with 0.04 g m^{-2} at ~9000 m). These values are low compared to the ones estimated by the LTM, possibly because of undersampling by the trawl gear (Gage and Bett, 2005). Belyaev (1989) also reported the estimates of benthic fauna abundance from two types of trawl samples recovered by the *Galathea* expedition from the Kermadec Trench: abundance was highest at the deepest site (2100 ind. m^{-2} at ~8200 m, compared with 63 to 1100 ind. m^{-2} at shallower hadal depth sites). The biomass increase with depth, predicted by our model, is generally consistent with these very limited data, and suggests that lateral transports of organic matter could explain the distribution pattern of benthic fauna in the Kermadec Trench.

5. Conclusions

We have developed a model that estimates the hadal benthic biomass as a function of vertical and lateral organic matter inputs, providing a broad-scale understanding of the potential effects of local topography on biomass distribution, and a quantitative theoretical framework to guide future sampling of trenches. Since early hadal exploration, unexpectedly high biomass levels found in some deep locations have suggested that benthic biomass might increase with depth in the trenches instead of decreasing as along other depth gradients. Lateral transport of food, and accumulation at depth, could be driving these trends.

Our outputs would allow, in the presence of a comprehensive hadal biomass dataset, constraining the lateral transport parameter (c) in the model. With this objective in mind, a survey should aim at sampling across the full depth range, and in areas with a range of estimated slope difference (ΔS), as this factor may be a key driver of food accumulation in trenches. Variations in the burial rate of organic matter only resulted in small differences in model outputs, suggesting that this factor might play a smaller role.

Trench topography appears to play a major role in determining areas of high benthic biomass: the presence of deep holes, opposed to a smooth and flat axis, is predicted to result in areas of higher biomass variability. Overall our model suggests that the simple process of lateral downslope sediment transport results in complex patterns of benthic biomass inside a trench.

Acknowledgments

We would like to thank Brian Bett and Andrew Yool for their useful comments and suggestions. MCI would also like to thank the University of Southampton, the Natural Environment Research Council (NERC, grant number NEW332003) and the Institute of Marine Engineering, Science & Technology (IMarEST), for supporting his research towards a PhD. We are grateful for the support provided by the National Science Foundation (OCE-1131620 to TMS, JCD, and PHY) to the Hadal Ecosystem Studies (HADES) project to which this paper forms a contribution. Support also came from the Natural Environment Research Council (NERC) and its Marine Environmental Mapping Programme (MAREMAP). Finally we would like to thank three anonymous reviewers for their useful comments and suggestions on how to improve our manuscript.

Appendix A

See. Tables A1 and A2 and Fig. A3.

Table A1
LTM output summary: means and standard deviations of four model outputs under 5 sets of model parameters of varying burial rate (B) and transport efficiency threshold (c), in relation to slope difference.

			Slope difference				Slope difference		
			Negative	Zero	Positive		Negative	Zero	Positive
Model run	B=4.5 ; c=6	**Lateral sediment input $g_{(ww)}$ m^{-2} y^{-1}**	0.5 (0.1)	0.6 (–)	3.7 (0.2)	**Sediment burial $g_{(ww)}$ m^{-2} y^{-1}**	0.1 (–)	0.1 (–)	0.1 (–)
	B=9 ; c=6		0.5 (0.1)	0.6 (–)	3.7 (0.2)		0.1 (–)	0.2 (–)	0.3 (–)
	B=18 ; c=6		0.5 (0.1)	0.6 (–)	3.7 (0.2)		0.2 (–)	0.4 (–)	0.5 (–)
	B=9 ; c=3		2.1 (0.3)	2.4 (0.1)	10.8 (0.5)		0.1 (–)	0.2 (–)	0.4 (–)
	B=9 ; c=12		0.1 (–)	0.1 (–)	0.8 (0.1)		0.2 (–)	0.2 (–)	0.2 (–)
Model run	B=4.5 ; c=6	**Mass of available food $g_{(ww)}$ m^{-2} y^{-1}**	3.9 (0.2)	6.9 (0.1)	9.6 (0.2)	**Biomass $g_{(ww)}$ m^{-2}**	26.7 (0.3)	30.3 (0.2)	34.9 (0.4)
	B=9 ; c=6		3.8 (0.1)	6.8 (0.1)	9.5 (0.2)		24.6 (0.3)	30.1 (0.2)	34.7 (0.4)
	B=18 ; c=6		3.7 (0.2)	6.6 (0.1)	9.2 (0.2)		24.3 (0.3)	29.7 (0.2)	34.3 (0.3)
	B=9 ; c=3		1.9 (0.1)	6.5 (0.1)	14.7 (0.6)		20.3 (0.3)	29.3 (0.2)	41.3 (0.8)
	B=9 ; c=12		5.5 (0.1)	6.9 (0.1)	7.0 (0.1)		28.1 (0.2)	30.3 (0.2)	30.7 (0.2)

Table A2
The slope (k), y-intercept (l) and x-intercept (m) of the linear regression of animal density ($y=\log_{10}$ (ind. m^{-2})) against the size range of benthic animals ($x=\log_{10}$ (g ind.$^{-1}$)) obtained under five different model scenarios of varying burial rate (B) and transport efficiency threshold (c). The regressions are calculated for areas of the trench with net sediment output (negative ΔS), equal inputs and outputs of sediment (zero ΔS) and net sediment input (positive ΔS). All the regressions have negative slope as the number of individuals per meter squared decreases when the nominal size of the individual increases. Furthermore the negative y-intercepts (l) suggest that animals heavier than 1 g are always present in abundances lower than 1 ind. m^{-2}. The x-intercept (m) gives the nominal size of the animals that, at each level of food input, reach a density of 1 ind. m^{-2}. The steepness of the regressions does not change between areas with different ΔS, nor between different model runs, suggesting that the density ratios between size classes remain constant notwithstanding the different levels of food availability. On the contrary, the height of the linear regression (i.e. x- and y-intercepts) changes with model run and ΔS, resulting in higher biomass and density in areas of higher food availability (i.e. positive ΔS).

$\log_{10}$(ind. m^{-2})$=k\times\log_{10}$(g ind.$^{-1}$)+l	**Negative ΔS**			**Zero ΔS**			**Positive ΔS**		
Model run	***k***	***l***	***m***	***k***	***l***	***m***	***k***	***l***	***m***
***B*=4 .5; *c*=6**	−0.733	−0.381	0.3018	−0.736	−0.252	0.4544	−0.737	−0.179	0.5716
***B*=9 ; *c*=6**	−0.733	−0.387	0.2960	−0.736	−0.255	0.4499	−0.737	−0.181	0.5675
***B*=18 ; *c*=6**	−0.735	−0.303	0.3873	−0.736	−0.262	0.4405	−0.737	−0.188	0.5550
***B*=9 ; *c*=3**	−0.722	−0.557	0.1693	−0.736	−0.265	2.2945	−0.737	−0.086	0.7651
***B*=9 ; *c*=12**	−0.735	−0.303	0.3873	−0.736	−0.252	0.4544	−0.736	−0.249	0.4591

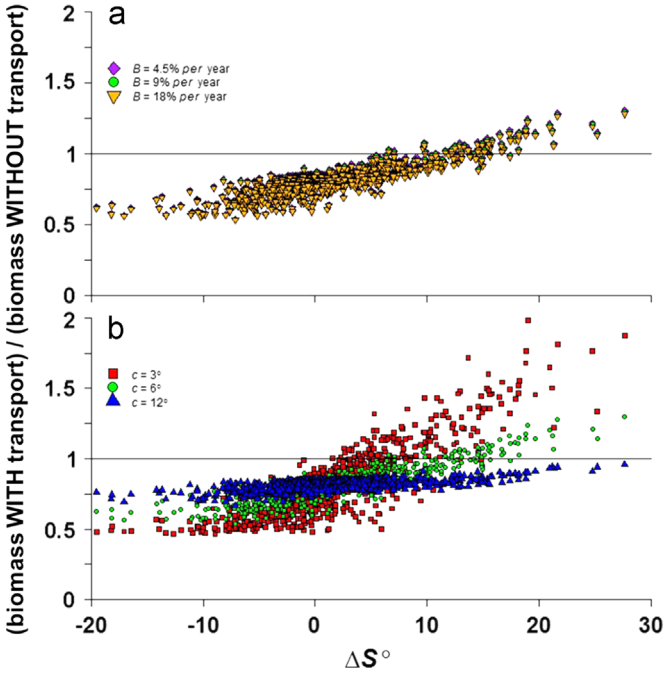

Fig. A3. The figure shows the change in modelled benthic biomass in the hadal area of the Kermadec Trench when introducing lateral transport, in relation to local topography (slope difference, ΔS°). The presence of lateral downslope transport results in higher benthic biomass levels than what would be expected in the absence of this process. A value of $y=1$ means "no change". Panel (a) shows three model runs with varying burial rate (B), and panel (b) shows three model runs with varying transport efficiency (c). The increase in expected benthic biomass is highest under high transport efficiency conditions, reaching a maximum increase factor of ~2. .

References

Belyaev, G.M., 1989. Deep-Sea Ocean Trenches and Their Fauna. Nauka Publishing House, Moscow.

Bendtsen, J., Lundsgaard, C., Middelboe, M., Archer, D., 2002. Influence of bacterial uptake on deep-ocean dissolved organic carbon. Global Biogeochem. Cycles 16, 4.

Bernhardt, M., Schultz, K., 2010. SnowSlide: a simple routine for calculating gravitational snow transport. Geophys. Res. Lett., 37.

Bernhardt, M., Schulz, K., Liston, G.E., Zangl, G., 2012. The influence of lateral snow redistribution processes on snow melt and sublimation in alpine regions. J. Hydrol. 424, 196–206.

Blankenship, L.E., Yayanos, A.A., Cadien, D.B., Levin, L.A., 2006. Vertical zonation patterns of scavenging amphipods from the Hadal zone of the Tonga and Kermadec Trenches. Deep Sea Res. I 53 (1), 48–61.

Canals, M., Puig, P., de Madron, X.D., Heussner, S., Palanques, A., Fabres, J., 2006. Flushing submarine canyons. Nature 444 (7117), 354–357.

Clark, M.R., Rowden, A.A., Schlacher, T., Williams, A., Consalvey, M., Stocks, K.I., Rogers, A.D., O'Hara, T.D., White, M., Shank, T.M., Hall-Spencer, J.M., 2010. The ecology of seamounts: structure, function, and human impacts. Annu. Rev. Mar. Sci., 253–278.

Danovaro, R., Della Croce, N., Dell'Anno, A., Pusceddu, A., 2003. A depocenter of organic matter at 7800 m depth in the SE Pacific Ocean. Deep Sea Res. II 50 (12), 1411–1420.

Danovaro, R., Gambi, C., Della Croce, N., 2002. Meiofauna hotspot in the Atacama Trench, eastern South Pacific Ocean. Deep Sea Res. I 49 (5), 843–857.

Duineveld, G.C.A., Lavaleye, M.S.S., Berghuis, E.M., 2004. Particle flux and food supply to a seamount cold-water coral community (Galicia Bank, NW Spain). Mar. Ecol. Prog. Ser. 277, 13–23.

ESRI, 2010. In: Institute), E.E.S.R. (Ed.), ArcGIS, Redlands, CA.

Fabiano, M., Pusceddu, A., Dell'Anno, A., Armeni, M., Vanucci, S., Lampitt, R.S., Wolff, G.A., Danovaro, R., 2001. Fluxes of phytopigments and labile organic matter to the deep ocean in the NE Atlantic Ocean. Prog. Oceanogr. 50 (1-4), 89–104.

Gage, J.D., Bett, B.J., 2005. Deep-sea Benthic Sampling.

Galeron, J., Sibuet, M., Mahaut, M.L., Dinet, A., 2000. Variation in structure and biomass of the benthic communities at three contrasting sites in the tropical Northeast Atlantic. Mar. Ecol. Prog. Ser. 197, 121–137.

Gallo, N.D., Cameron, J., Hardy, K., Fryer, P., Bartlett, D.H., Levin, L.A., 2015. Submersible and lander-observed community patterns in the Mariana and New Britain Trenches: influence of productivity and depth on epibenthic community structure. Deep Sea Res. I.

Gardner, J.V., Armstrong, A.A., Calder, B.R., Beaudoin, J., 2014. So, how deep is the Mariana Trench? Geology 37 (1), 1–13.

George, R.Y., Higgins, R.P., 1979. Eutrophic hadal benthic community in the Puerto Rico Trench. Ambio Spec. Rep. 6, 51–58.

Glud, R.N., Wenzhöfer, F., Middelboe, M., Oguri, K., Turnewitsch, R., Canfield, D.E., Kitazato, H., 2013. High rates of microbial carbon turnover in sediments in the deepest oceanic trench on Earth. Nat. Geosci. 6 (4), 284–288.

Griesbach, S., Peters, R.H., Youakim, S., 1982. An allometric model for pesticide bioaccumulation. Can. J. Fish. Aquat. Sci. 39 (5), 727–735.

Higgs, N.D., Gates, A.R., Jones, D.O.B., 2014. Fish food in the deep sea: revisiting the role of large food-falls. PLoS One 9, 5.

Honjo, S., Manganini, S.J., Krishfield, R.A., Francois, R., 2008. Particulate organic carbon fluxes to the ocean interior and factors controlling the biological pump: a synthesis of global sediment trap programs since 1983. Prog. Oceanogr. 76 (3), 217–285.

Inman, D.L., Nordstrom, C.E., Flick, R.E., 1976. Currents in submarine canyons—air–sea–land interaction. Annu. Rev. Fluid Mech. 8, 275–310.

Itoh, M., Kawamura, K., Kitahashi, T., Kojima, S., Katagiri, H., Shimanaga, M., 2011. Bathymetric patterns of meiofaunal abundance and biomass associated with the Kuril and Ryukyu trenches, western North Pacific Ocean. Deep Sea Res. I 58 (1), 86–97.

Itou, M., Matsumura, I., Noriki, S., 2000. A large flux of particulate matter in the deep Japan Trench observed just after the 1994 Sanriku-Oki earthquake. Deep Sea Res. I 47 (10), 1987–1998.

Jamieson, A.J., Fujii, T., Mayor, D.J., Solan, M., Priede, I.G., 2010. Hadal trenches: the ecology of the deepest places on Earth. Trends Ecol. Evol. 25 (3), 190–197.

Jamieson, A.J., Fujii, T., Solan, M., Matsumoto, A.K., Bagley, P.M., Priede, I.G., 2009. First findings of decapod crustacea in the hadal zone. Deep Sea Res. I 56 (4), 641–647.

Jamieson, A.J., Kilgallen, N.M., Rowden, A.A., Fujii, T., Horton, T., Loerz, A.N., Kitazawa, K., Priede, I.G., 2011. Bait-attending fauna of the Kermadec Trench, SW Pacific Ocean: evidence for an ecotone across the abyssal-hadal transition zone. Deep Sea Res. II 58 (1), 49–62.

Jamieson, A.J., Lace, N.C., Lörz, A.-N., Rowden, A.A., Piertney, S.B., 2013. The supergiant amphipod Alicella gigantea (Crustacea: Alicellidae) from hadal depths in the Kermadec Trench, SW Pacific Ocean. Deep Sea Res. II 92, 107–113.

Jamieson, A.J., Yancey, P.H., 2012. On the validity of the trieste flatfish: dispelling the myth. Biol. Bull. 222 (3), 171–175.

Johnson, N.A., Campbell, J.W., Moorre, T.S., Rex, M.A., Etter, R.J., McClain, C.R., Dowell, M.D., 2007. The relationship between the standing stock of deep-sea macrobenthos and surface production in the western North Atlantic. Deep Sea Res. I 54 (8), 1350–1360.
Kelly-Gerreyn, B.A., Martin, A.P., Bett, B.J., Anderson, T.R., Kaariainen, J.I., Main, C.E., Marcinko, C.J., Yool, A., 2014. Benthic biomass size spectra in shelf and deep-sea sediments. Biogeosciences 11 (22), 6401–6416.
Kelly, R.H., Yancey, P.H., 1999. High contents of trimethylamine oxide correlating with depth in deep-sea teleost fishes, skates, and decapod crustaceans. Biol. Bull. 196 (1), 18–25.
Laxson, C.J., Condon, N.E., Drazen, J.C., Yancey, P.H., 2011. Decreasing urea: trimethylamine N-oxide ratios with depth in chondrichthyes: a physiological depth limit? Physiol. Biochem. Zool. 84 (5), 494–505.
Lebrato, M., Pitt, K.A., Sweetman, A.K., Jones, D.O.B., Cartes, J.E., Oschlies, A., Condon, R.H., Molinero, J.C., Adler, L., Gaillard, C., Lloris, D., Billett, D.S.M., 2012. Jelly-falls historic and recent observations: a review to drive future research directions. Hydrobiologia 690 (1), 227–245.
Longhurst, A., Sathyendranath, S., Platt, T., Caverhill, C., 1995. An estimate of global primary production in the ocean from satellite radiometer data. J. Plankton Res. 17 (6), 1245–1271.
Lutz, M.J., Caldeira, K., Dunbar, R.B., Behrenfeld, M.J., 2007. Seasonal rhythms of net primary production and particulate organic carbon flux to depth describe the efficiency of biological pump in the global ocean. J. Geophys. Res. Oceans 112 (C10).
Martin, J.H., Knauer, G.A., Karl, D.M., Broenkow, W.W., 1987. VERTEX—carbon cycling in the northeast Pacific. Deep Sea Res. Part A 34 (2), 267–285.
Mayor, D.J., Thornton, B., Hay, S., Zuur, A.F., Nicol, G.W., McWilliam, J.M., Witte, U.F. M., 2012. Resource quality affects carbon cycling in deep-sea sediments. ISME J. 6 (9), 1740–1748.
McGillicuddy, D.J., Robinson, A.R., Siegel, D.A., Jannasch, H.W., Johnson, R., Dickey, T.D., McNeil, J., Michaels, A., Knap, A.H., 1998. Influence of mesoscale eddies in new production in the Sargasso sea. Nature 394 (6690), 263–266.
Middelburg, J.J., 2011. Chemoautotrophy in the ocean. Geophys. Res. Lett., 38.
Olu, K., Lance, S., Sibuet, M., Henry, P., FialaMedioni, A., Dinet, A., 1997. Cold seep communities as indicators of fluid expulsion patterns through mud volcanoes seaward of the Barbados accretionary prism. Deep Sea Res. II 44 (5), 811–841.
Peters, R.H., 1983. Cambridge Studies In Ecology: The Ecological Implications of Body Size. Cambridge University Press, New York, NY, USA.
R Core Team , 2012. R: A Language and Environment for Statistical Computing. R Foundation for Statistical Computing, Vienna, Austria.
Reimers, C.E., Jahnke, R.A., McCorkle, D.C., 1992. Carbon fluxes and burial rates over the continental slope and rise off central California with implications for the global carbon cycle. Global Biogeochem. Cycles 6 (2), 199–224.
Rex, M.A., Etter, R.J., 2010. Deep-sea Biodiversity: Pattern and Scale. Harvard University Press, Cambridge & London.
Rex, M.A., Etter, R.J., Morris, J.S., Crouse, J., McClain, C.R., Johnson, N.A., Stuart, C.T., Deming, J.W., Thies, R., Avery, R., 2006. Global bathymetric patterns of standing stock and body size in the deep-sea benthos. Mar. Ecol. Prog. Ser. 317, 1–8.
Richardson, M.D., Briggs, K.B., Bowles, F.A., Tietjen, J.H., 1995. A depauperate benthic assemblage from the nutrient-poor sediments of the Puerto-Rico Trench. Deep Sea Res. I 42 (3), 351–364.
Rowden, A.A., Dower, J.F., Schlacher, T.A., Consalvey, M., Clark, M.R., 2010. Paradigms in seamount ecology: fact, fiction and future. Mar. Ecol. Evol. Perspect. 31, 226–241.
Ruhl, H.A., Bett, B.J., Hughes, S.J.M., Alt, C.H.S., Ross, E.J., Lampitt, R.S., Pebody, C.A., Smith, K.L., Billet, D.S.M., 2014. Links between deep-sea respiration and community dynamics. Ecology 95 (6), 1651–1662.
Ruhl, H.A., Ellena, J.A., Smith Jr., K.L., 2008. Connections between climate, food limitation, and carbon cycling in abyssal sediment communities. Proc. Natl. Acad. Sci. U.S.A. 105 (44), 17006–17011.
Schmidt, W.E., Siegel, E., 2011. Free descent and on bottom ADCM measurements in the Puerto Rico Trench, 19.77 degrees N, 67.40 degrees W. Deep Sea Res. I 58 (9), 970–977.
Smith, C.R., Baco, A.R., 2003. Ecology of whale falls at the deep-sea floor. Oceanogr. Mar. Biol. 41, 311–354.
Smith, K.L., Ruhl, H.A., Kahru, M., Huffard, C.L., Sherman, A.D., 2013. Deep ocean communities impacted by changing climate over 24 y in the abyssal northeast Pacific Ocean. Proc. Natl. Acad. Sci. U.S.A. 110 (49), 19838–19841.
Suess, E., 1980. Particulate organic-carbon flux in the oceans—surface productivity and oxygen utilization. Nature 288 (5788), 260–263.
Sweetman, A.K., Witte, U., 2008. Response of an abyssal macrofaunal community to a phytodetrital pulse. Mar. Ecol. Prog. Ser. 355, 73–84.
Thresher, R.E., Adkins, J., Fallon, S.J., Gowlett-Holmes, K., Althaus, F., Williams, A., 2011. Extraordinarily high biomass benthic community on Southern Ocean seamounts. Sci. Rep., 1.
Thurston, M.H., Rice, A.L., Bett, B.J., 1998. Latitudinal variation in invertebrate megafaunal abundance and biomass in the North Atlantic Ocean Abyss. Deep Sea Res. II 45 (1-3), 203–224.
Tietjen, J.H., Deming, J.W., Rowe, G.T., Macko, S., Wilke, R.J., 1989. Meiobenthos of the Hatteras abyssal-plain and Puerto-Rico trench—abundance, biomass and association with bacteria and particulate fluxes. Deep Sea Res. Part A 36 (10), 1567–1577.
Tselepides, A., Lampadariou, N., 2004. Deep-sea meiofaunal community structure in the Eastern Mediterranean: are trenches benthic hotspots? Deep Sea Res. I 51 (6), 833–847.
Turnewitsch, R., Falahat, S., Nycander, J., Dale, A., Scott, R.B., Furnival, D., 2013. Deep-sea fluid and sediment dynamics—influence of hill- to seamount-scale seafloor topography. Earth-Sci. Rev. 127, 203–241.
Turnewitsch, R., Falahat, S., Stehlikova, J., Oguri, K., Glud, R.N., Middelboe, M., Kitazato, H., Wenzhöfer, F., Ando, K., Fujio, S., Yanagimoto, D., 2014. Recent sediment dynamics in hadal trenches: evidence for the influence of higher-frequency (tidal, near-inertial) fluid dynamics. Deep Sea Res. I 90, 125–138.
Venables, H.J., Pollard, R.T., Popova, E.E., 2007. Physical conditions controlling the development of a regular phytoplankton bloom north of the Crozet Plateau, Southern Ocean. Deep Sea Res. Part II 54 (18-20), 1949–1965.
Vetter, E.W., Dayton, P.K., 1998. Macrofaunal communities within and adjacent to a detritus-rich submarine canyon system. Deep Sea Res. Part II 45 (1-3), 25–54.
Vinogradova, N.G., Gebruk, A., Romanov, V.N., 1993. Some new data on the orkney trench ultra abyssal fauna. In: The Second Polish-Soviet Antarctic Symposium. Institute of Ecology. Publishing Office, pp. 213–221.
Wolff, T., 1961. The deepest recorded fishes. Nature 190 (4772), 283.
Wolff, T., 1970. Concept of hadal or ultra-abyssal fauna. Deep Sea Res. 17 (6), 983–1003.
Yancey, P.H., Gerringer, M.E., Drazen, J.C., Rowden, A.A., Jamieson, A.J., 2014. Marine fish may be biochemically constrained from inhabiting deepest ocean depths. Proc. Natl. Acad. Sci. U.S.A. 111, 4461–4465.